

# Primary results of glaciological studies along an 1100 km transect from Zhongshan station to Dome A, East Antarctic ice sheet

QIN DAHE,<sup>1</sup> REN JIAWEN,<sup>1</sup> KANG JIANCHENG,<sup>2</sup> XIAO CUNDE,<sup>1</sup> LI ZHONGQIN,<sup>1</sup> LI YUANSHEG,<sup>2</sup>  
SUN BO,<sup>2</sup> SUN WEIZHEN,<sup>1</sup> WANG XIAOXIANG<sup>1</sup>

<sup>1</sup>Laboratory of Ice Core and Cold Regions Environment, Lanzhou Institute of Glaciology and Geocryology,  
Chinese Academy of Sciences, Lanzhou, Gansu 730000, China

<sup>2</sup>Polar Research Institute of China, Shanghai, 200129, China

**ABSTRACT.** The Chinese National Antarctic Research Expedition (CHINARE) carried out three traverses from Zhongshan station to Dome A, Princess Elizabeth Land and Inaccessible Area, East Antarctic ice sheet, during the 1996/97 to 1998/99 Antarctic field seasons. The expeditions are part of the Chinese International Trans-Antarctic Scientific Expedition program. In this project, glaciological investigations of mass balance, ice temperature, ice flow, stratigraphy in snow pits and snow/firn ice cores, as well as the glaciochemical study of surface snow and shallow ice cores, have been carried out. In the 1998/99 field season, CHINARE extended the traverse route to 1128 km inland from Zhongshan station. The density profiles show that firnification over Princess Elizabeth Land and Inaccessible Area (290–1100 km along the route) is fairly slow, and the accumulation rate recovered from snow pits along the initial 460 km of the route is 4.6–21 cm (46–210 kg m<sup>-2</sup> a<sup>-1</sup>) water equivalent. The initial 460 km of the route can be divided into four sections based on the differences of accumulation rate. This pattern approximately coincides with the study on the Lambert Glacier basin (LGB) by Australian scientists. During the past 50 years, the trends of both air temperature and accumulation rate show a slight increase in this area, in contrast to the west side of the LGB. Data on surface accumulation rates and their spatial and temporal variability over ice-drainage areas such as the LGB are essential for precise mass-balance calculation of the whole ice sheet, and are important for driving ice-sheet models and testing atmospheric models.

## INTRODUCTION

In the framework of the International Trans-Antarctic Scientific Expedition (ITASE) and Chinese Antarctic glaciological research program, glaciological studies have been conducted along the transect from Zhongshan station to Dome A. The first traverse expedition was carried out to a point 296 km inland from Zhongshan station during the 1996/97 austral summer (13th Chinese National Antarctic Research Expedition (CHINARE)). The traverse was extended southwards to 464 km during the 1997/98 (14th CHINARE) and to 1128 km during the 1998/99 (15th CHINARE) field season. The accumulation rate was recovered from stake measurements, snow pits and shallow firn cores (50–100 m). Stable-isotope and chemical records were also determined for the snow pits and firn cores. Radio-echo sounding was carried out along the 1128 km route during the 1998/99 expedition, but the results are not yet available.

The initial 294 km of the route is partly coincident with the Australian National Antarctic Research Expeditions (ANARE) traverse route surrounding the Lambert Glacier

basin (LGB). In the 1993/94 and 1994/95 field seasons, the LGB oversnow traverse program covered the routes from the west to the east side of the LGB and terminated at LGB72, which is 68 km from Zhongshan station. As the main component in calculating the mass budget for the LGB drainage basin, the surface mass balance over this region was estimated by Allison (1979) and McIntyre (1985) from isolated measurements and interpretation of satellite imagery, respectively. Over the section from LGB72 to LGB65 (294 km from Zhongshan station), surface accumulation, snow density, 10 m firn temperature and  $\delta^{18}\text{O}$  measurements were conducted during the ANARE traverse.

Investigations of the surface mass balance over the vast ice sheet are still relatively scarce, and mass-balance studies over ice-drainage areas such as the LGB are essential for precise mass-balance calculation for the whole ice sheet. The data on surface accumulation rates and their spatial and temporal variability are important for driving ice-sheet models and testing atmospheric models. The route of the Chinese traverse is mainly located in Princess Elizabeth Land and Inaccessible Area. Up to now, there has been little glaciological investigation of the regions covered by the final 550 km of the route. In this paper, the spatial variation of snow density and the surface accumulation rate over the initial 294 km of the route are presented, and the data for the initial 294 km

\* Now Cold and Arid Regions Environmental and Engineering Research Institute.

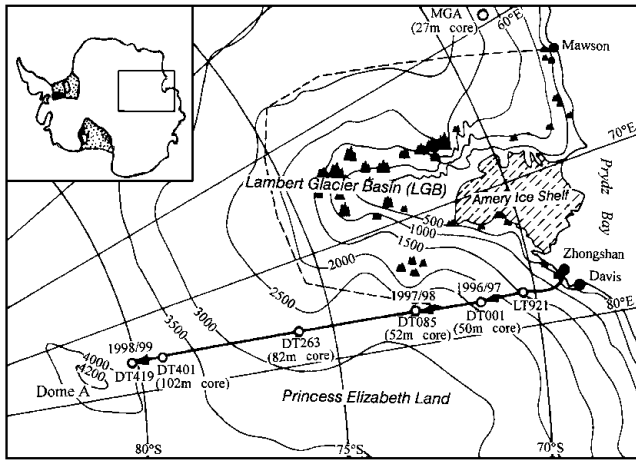


Fig. 1. Sketch map showing the route of the Chinese Antarctic inland traverses during the years 1996–99. Circles represent the locations where ice/firn cores and snow-pit samples discussed in the text, were obtained. The dashed line is the ANARE traverse route.

compared with those obtained by ANARE. Snow-chemistry analyses were conducted for snow pits and firn cores, of which only the results from the first traverse are shown.

**SAMPLING AND EXPERIMENTAL PROCEDURES**

Figure 1 shows the area under investigation, with the five drilling sites of the 27–102 m deep firn cores at DT001 (50 m), DT085 (52 m), DT263 (82 m), DT401 (102 m) and MGA (27 m). Two snow-pit sites, at LT921 (2.2 m) and DT001 (3.2 m) on the east side of the LGB, are also shown. The MGA firn core was extracted during the 1992/93 ANARE traverse, which included one of the authors (Good-

win and others, 1994; Ren and others, 1999). Snow pits were sampled every 3 cm along one of the pit walls. The firn cores at DT001 and MGA were also resampled every 3 cm in the cold storage at the Lanzhou Institute of Glaciology and Geocryology, China.

All samples were kept frozen until processed. Concentrations of major cations and anions were measured by Dionex-300 and Dionex-100 ion chromatography, respectively. The detection limits and precision, respectively, were  $1 \times 10^{-6} \text{ g g}^{-1}$  and  $\pm 5\%$  for  $\text{Na}^+$ ,  $\text{Cl}^-$  and  $\text{SO}_4^{2-}$ , and  $1 \times 10^{-6} \text{ g g}^{-1}$  and  $\pm 20\%$  for  $\text{Ca}^{2+}$ . The  $\delta^{18}\text{O}$  measurements were done by MAT-252 Gas Stable Isotope Ratio Mass Spectrometer, with respect to standard mean ocean water measurement, to a precision of  $\pm 0.5\text{‰}$ .

**ISOTOPE AND CHEMISTRY PROFILES AND DATING OF SNOW PITS AND FIRN CORES**

Reliable chronologies are the first step for snow/ice-core studies. Various methods can be used to provide dating of depth profiles. These include stratigraphic studies, reference horizons, radioactive decay of some radionuclides and comparison with other records. In principle, numerous stratigraphical methods based on seasonal changes in the isotopic composition of the ice or in the concentration of impurities, as well as in physical properties of snow, may be used to establish year-to-year dating of ice cores.

The chemical profiles from the LT921 and DT001 snow pits, as well as the upper layers of the DT001 firn core, show that  $\delta^{18}\text{O}$ ,  $\text{Cl}^-$ ,  $\text{Na}^+$  and  $\text{NO}_3^-$  have clear seasonal variations, and thus provide a relatively reliable basis for the dating of snow pits or firn cores in this region (Fig. 2a and b). Among the chemical species currently measured in polar snow layers, it appears that sodium and chloride exhibit very strong seasonal cycles. For instance, concentrations of sodium (a good tracer of sea salt) exhibit large variations (a

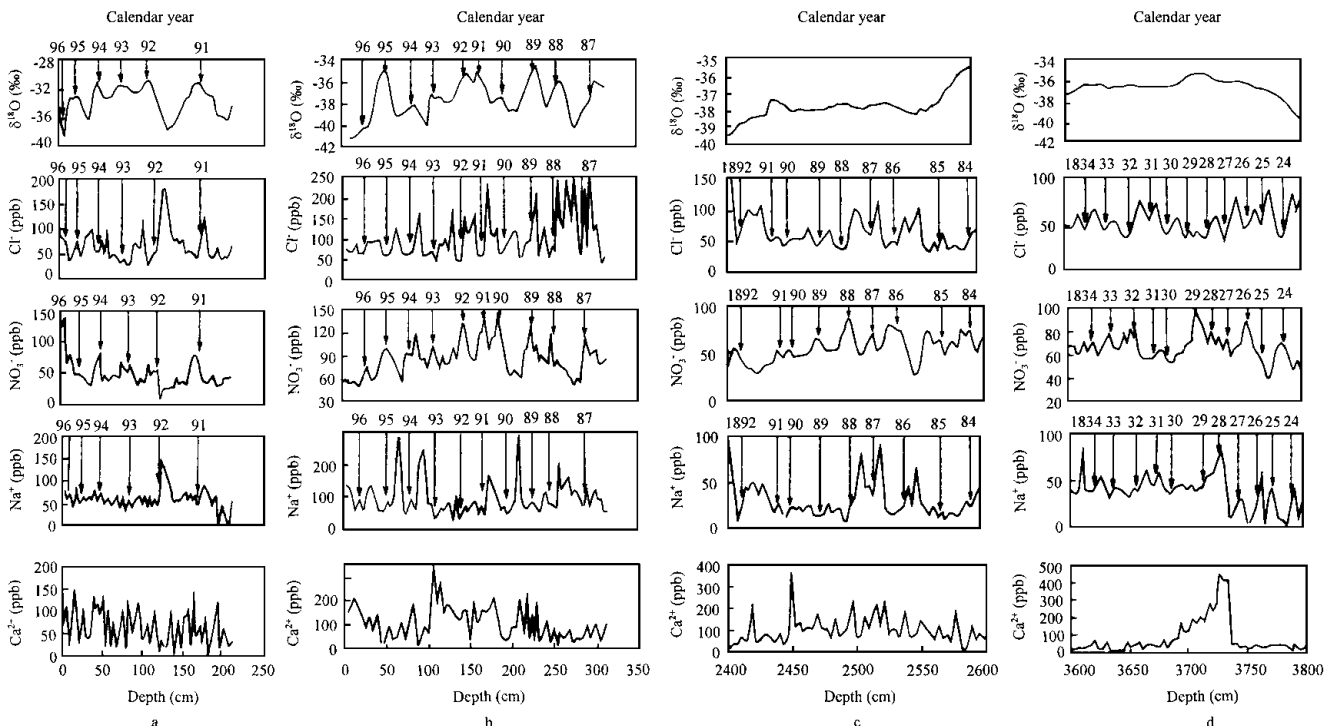


Fig. 2.  $\delta^{18}\text{O}$ ,  $\text{Cl}^-$ ,  $\text{Na}^+$ ,  $\text{NO}_3^-$  and  $\text{Ca}^{2+}$  profiles in snow pits at LT921 (a) and DT001 (b) covering the periods 1991–96 and 1984–96, respectively; and in firn cores at DT001 covering depths 24–26 m (c) and 36–38 m (d).

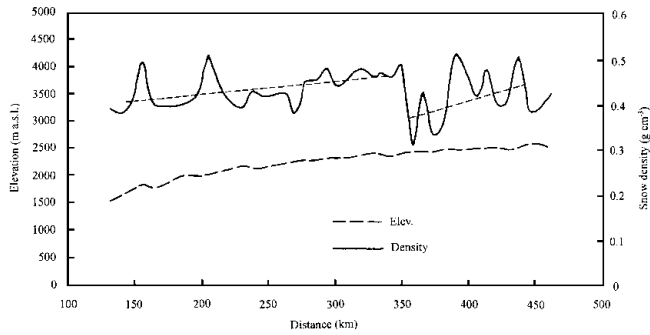


Fig. 3. The distribution of the upper 0.2 m snow density measured at about 8 km intervals along the initial 450 km of the traverse route (measurement starts from 130 km south of Zhongshan).

winter to summer ratio of 5–10) in Antarctic snow layers, due to frequent advection of marine air masses in winter over the ice sheet (Herron, 1982). Because an additional input of hydrochloric acid takes place in summer, the seasonal variation of chloride is weaker than that of sodium. Besides these two species, acidic species like nitrate and sulfate exhibit moderate maxima in summer and spring in Antarctic snow layers. The accuracy of the dating is much increased when several parameters are considered together. It is clear from Figure 2 that the variations of  $\text{NO}_3^-$  are partly in phase with those of  $\delta^{18}\text{O}$ , while the variations of  $\text{Cl}^-$  and  $\text{Na}^+$  are in anti-phase with those of  $\delta^{18}\text{O}$ , except for the sodium record in Figure 2a, which shows no clear correlation. However, the seasonal variations of  $\delta^{18}\text{O}$  are gradually smoothed below 3 m (corresponding to about ten annual layers), while the seasonal variations of  $\text{Cl}^-$ ,  $\text{Na}^+$  and  $\text{NO}_3^-$  are fairly consistent throughout the profile of the 50 m firn core (about 250 annual layers; Fig. 2c and d). No obvious seasonal variations of  $\text{Ca}^{2+}$  are found in the snow-pit profiles and the firn core.

### DENSITY

Snow density was measured by weighing the samples collected using a hollow steel tube with a volume of  $10\text{ cm} \times 10\text{ cm} \times 2\text{ cm}$ . The density of the upper 0.2 m of snow was measured at about 8 km intervals 130–450 km along the traverse route (Fig. 3). In the section from 130 to 350 km the surface density is relatively stable ( $0.4\text{--}0.5\text{ g cm}^{-3}$ ), while from 350 to 450 km it displays considerable spatial variations, although most values are still in the range  $0.4\text{--}0.5\text{ g cm}^{-3}$ . This is because katabatic winds dominate at 2500–3000 m a.s.l., and as a result sastrugi 30 cm high or more are widespread in this section. The surface roughness in this latitudinal range is much larger than in other sections of the route. Wind speed is a key factor for the formation of the surface roughness over the vast ice sheet. The annual mean wind speed for 1995 recorded by an automatic weather station (AWS) installed at LGB59 (2537 m a.s.l.), close to DT085 (2577 m a.s.l.), is  $9.7\text{ m s}^{-1}$ . At the coastal Zhongshan station, the annual mean for 1995 is  $7.3\text{ m s}^{-1}$ , although the anemometer height at Zhongshan is actually higher than at LGB59. Simultaneous observations during the traverse also indicated higher wind speeds ( $9\text{--}12\text{ m s}^{-1}$ ) in this section than in the lower or higher latitudinal ranges ( $6\text{--}10\text{ m s}^{-1}$ ). Craven and Allison (1998) examined the dependence of firnification on temperature, wind and accumulation rate using two empirical models, based on firn-core data from widely spread Antarctic sites. They showed that a  $5\text{ m s}^{-1}$  wind-speed increase has an effect equivalent to that of a  $10^\circ\text{C}$  temperature increase, or a  $0.1\text{ m a}^{-1}$  accumulation-rate decrease. Strong wind has an obvious effect in increasing the firnification rate.

The surface density was also measured over the upper 1 m of firn, with a 2 cm sampling interval. The density profiles are quite stable, in the range  $0.35\text{--}0.45\text{ g cm}^{-3}$  (Fig. 4). Generally, before the density reaches  $0.55\text{ g cm}^{-3}$ , the densification process is dominated by grain-settling, sublimation/condensation, volume/surface diffusion as well as recrystallization. Since the process does not involve meltwater in the interior

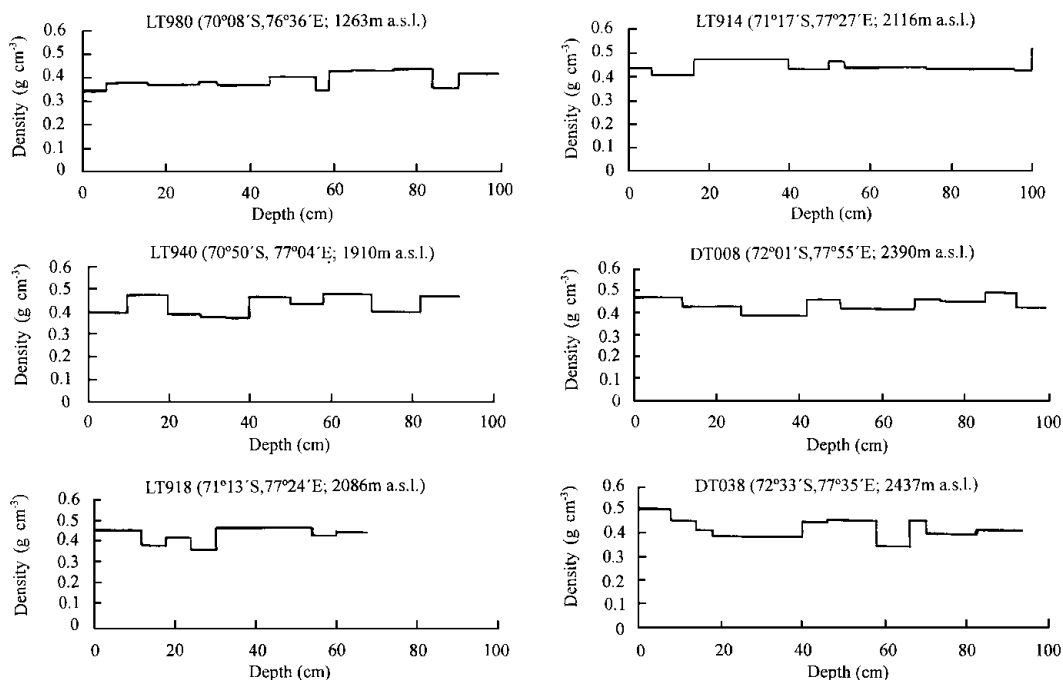


Fig. 4. Density profiles in the upper 1 m of snow at six sites over the northern 464 km section of the line.

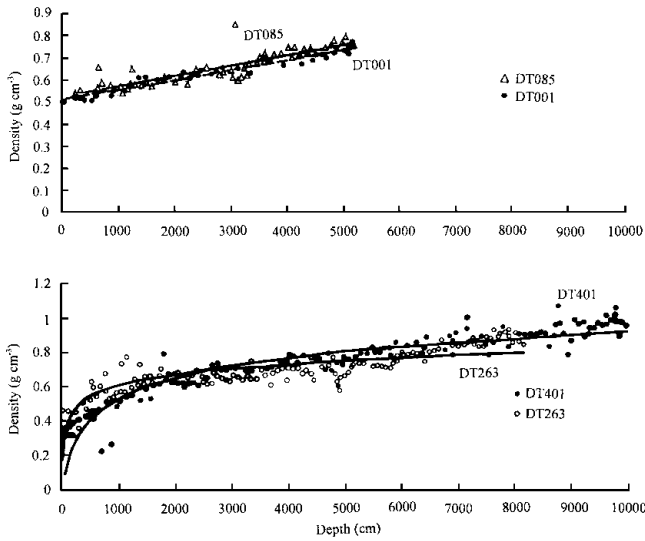


Fig. 5. Density profiles in the firn cores drilled at DT001, DT085, DT263 and DT401.

of the Antarctic ice sheet, it is so-called “dry densification”. Qin (1990) classified it as cold-type densification, characterized by a primary mechanism of sintering, which occurs over the vast central regions of Antarctica (the northern limit is approximately 100 km inland from the coast) where the annual temperature is  $< -25^{\circ}\text{C}$ , with a maximum of  $< 0^{\circ}\text{C}$ . Wind speed plays an important role during dry densification of the surface layer of snow, while another important factor may be the annual mean temperature. The role of the overburden pressure is negligible in such shallow layers. Since strong wind over Princess Elizabeth Land runs towards the LGB all the year round, the snowfall in almost all seasons can rapidly be packed onto the surface of the ice sheet by the wind. Therefore, the seasonal variation in density is not obvious with a sampling resolution of 2 cm.

Continuous density measurement was carried out on the firn cores drilled at DT001, DT085, DT263 and DT401 (Fig. 5). Probably because of the enhanced densification in upper layers, resulting from the high wind speed, linear regressions of the density vs depth for the firn core at DT001 and

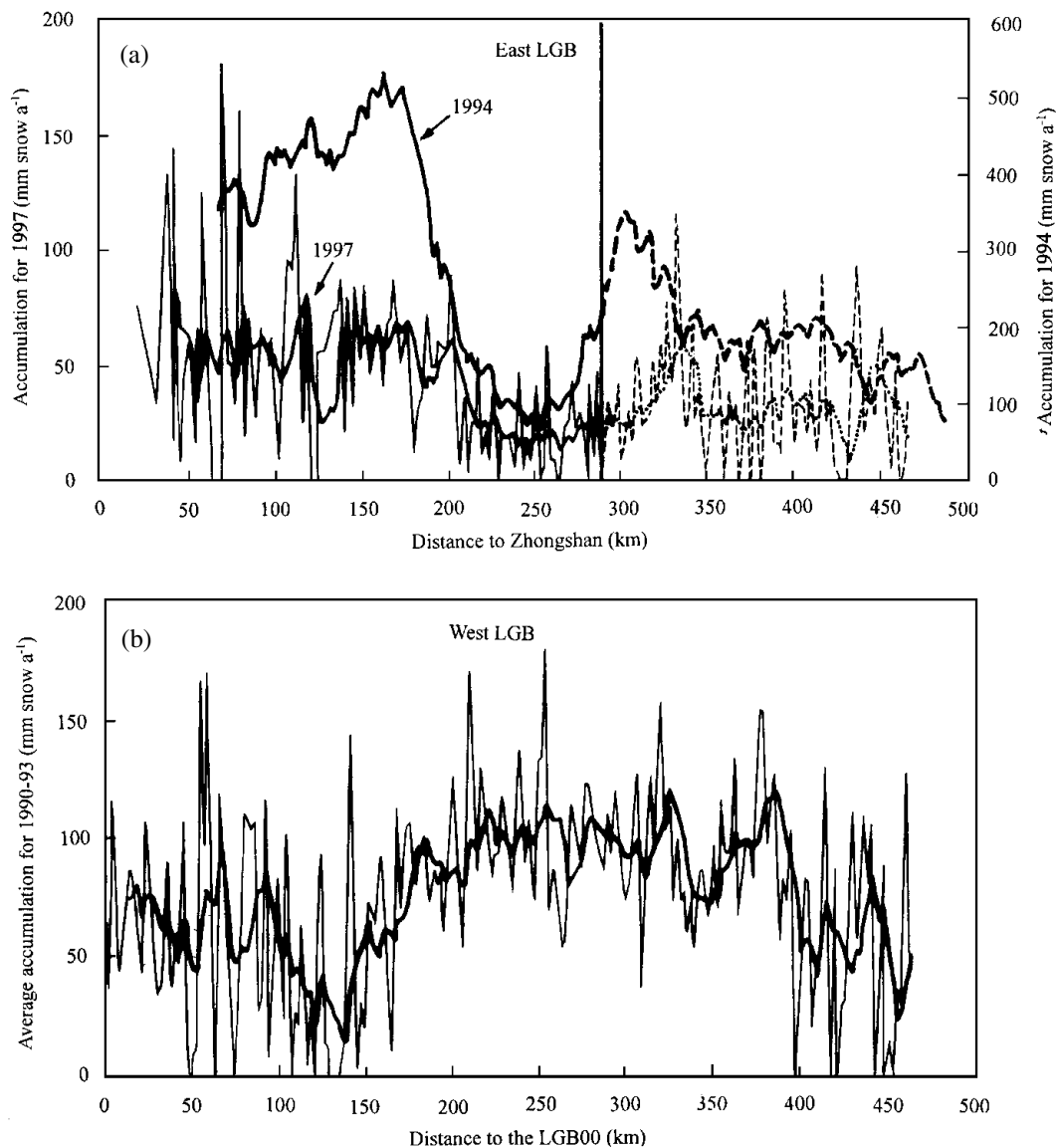


Fig. 6. The distribution of the annual accumulation rate in 1997 along the initial 460 km of the traverse lines on both sides of the LGB. The seven-point-smoothed profiles give the trends of spatial variations (bold lines). The value for 1994 over the eastern LGB is the 30 km unweighted mean of the measuring sites (Higham and Craven, 1997). (a) The two traverse lines conducted by CHINARE and ANARE separate after 294 km; the accumulation over this section is shown by dashed profiles. (b) The start point (LGB00) lies 130 km inland of the coast.

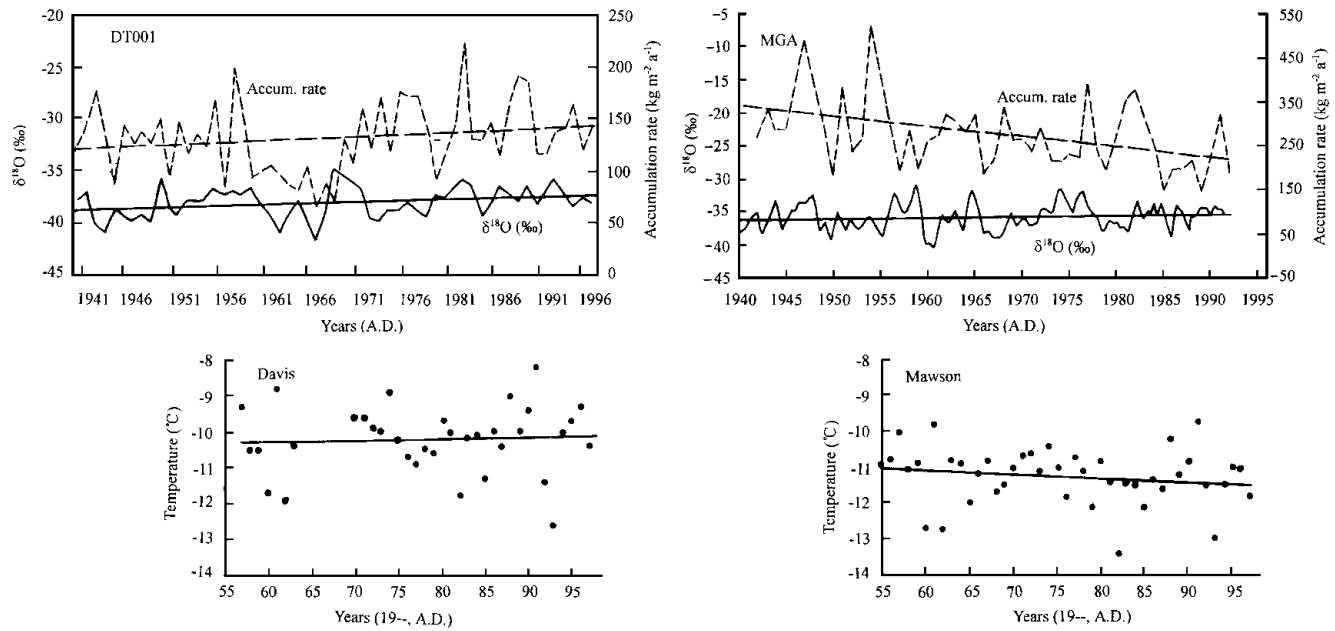


Fig. 7. Contrast of the annual accumulation rate and  $\delta^{18}\text{O}$  profiles between firn cores at DT001 (east LGB) and MGA (west LGB), both covering the past 50 years. The  $\delta^{18}\text{O}$  profile for MGA is seven-point smoothed in order to give a comparable trend with that of accumulation rate. Instrumental temperature records at Davis station (east coast of LGB) and Mawson station (west coast of LGB) are illustrated, covering the period from the mid-1950s to 1996.

DT085 are a better fit than logarithmic functions. The same finding was made over the inland region of the western LGB (Craven and Allison, 1998). However, for the 80 m core at DT263 and the 100 m core at DT401, good logarithmic correlations were established ( $r = 0.80$  and  $0.93$ , respectively). The depth of pore close-off (corresponding to a density of  $0.83 \text{ g cm}^{-3}$ ) is around 60 m at both DT263 and DT401. If the regression lines are extended for the density profiles of DT001 and DT085, the depth of the value  $0.83 \text{ g cm}^{-3}$  is also around 60 m. This means that the densification process in this large region (290–1100 km along the route), is fairly slow, as at other interior Antarctic sites.

### SPATIAL AND TEMPORAL VARIATIONS OF ACCUMULATION RATE

Individual measurements of surface mass balance were made on bamboo canes spaced at 2 km intervals along the whole traverse route. For the section from 460 to 1128 km, only initial values of the cane height are available, so the accumulation rate cannot be calculated yet. The annual mean accumulation rate for 1997 along the coastal 460 km is plotted in Figure 6a. The seven-point-smoothed profile gives the trend of the spatial variation. It displays relatively high values (up to  $200 \text{ mm a}^{-1}$ ) of snow accumulation for the initial 200 km, and then declines and remains stable ( $0\text{--}100 \text{ mm a}^{-1}$ ) further south, with a few individual sites having below-zero accumulation. This spatial variation is compared with the annual accumulation measured by ANARE in 1994 along a partly coincident route (LGB72 to LT782; Higham and Craven, 1997). The two profiles display similar spatial trends, but with the average values for 1994 over three times higher than those for 1997, which may imply a much higher precipitation in 1994. However, in the section south of 294 km the two lines separate, leading to different spatial trends.

The same study was performed by Australian scientists on the west side of the LGB (Goodwin and others, 1994; Higham and others, 1997). In Figure 6b, surface accumulation rate in the 460 km section from LGB00 to LGB20 (site LGB00 is 130 km inland) in the western LGB is plotted. The values are the annual accumulation rates averaged for the years 1990–93. The values over the first 150 km are roughly in the range  $0\text{--}120 \text{ mm a}^{-1}$  (with a few sites below zero), while in the section from 150 to 400 km they are  $60\text{--}160 \text{ mm a}^{-1}$ , and in the section from 400 to 460 km they are  $0\text{--}120 \text{ mm a}^{-1}$  again. It has long been considered that the accumulation rates on the two sides of the LGB are quite different. Higham and others (1997) believe that the difference is caused by dominant southeasterly wind fields under the combined influence of katabatic and geostrophic flows. Allison (1998) suggests that the accumulation rate on the eastern LGB is up to 50% less than at the equivalent elevation on the western side due to the “rain-shadow” effect of the prevailing upper-level winds.

Presumably, the difference in spatial variations between the eastern and western LGB is due to the difference in the main vapor-transport paths. On the west side of the LGB, the flattest region is around the head of Amery Ice Shelf, from where the vapor could be transported most efficiently, while the steep coast near Mawson station makes for less efficient transport. This would explain the higher accumulation in the middle of the western LGB traverse line, and the lower accumulation over the initial section. On the east side, by contrast, the topography is steep in all directions inland from the LGB, and the coastal area is the most favorable direction for vapor transportation, leading to the declining trend of accumulation inland from the coast. Short-distance variation of accumulation is closely related to the micro-relief.

The accumulation rates were also recovered from several snow pits along the initial 500 km of the route, giving values in the range  $4.6\text{--}21 \text{ cm}$  ( $46\text{--}210 \text{ kg m}^{-2} \text{ a}^{-1}$ ) water equivalent. The initial 500 km of the route can be divided into four sub-



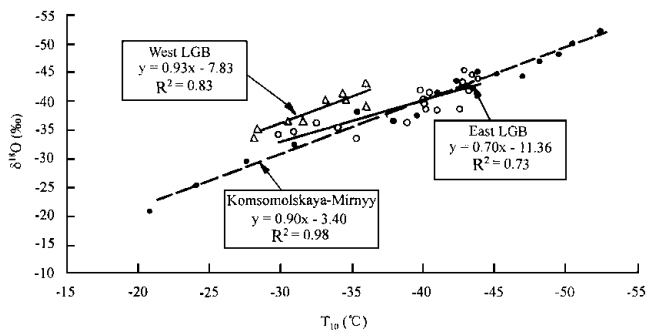


Fig. 8. Correlation of  $\delta^{18}\text{O}$  vs  $T_{10}$  along the two sides of the LGB, compared with the results obtained between Komsomolskaya and Mirny during the 1990 ITAE (Qin and others, 1994).

sections based on the accumulation-rate differences. The accumulation rate is highest on the section from 0 to 65 km ( $140\text{--}210\text{ kg m}^{-2}\text{ a}^{-1}$ ); still high in the section from 65 to 140 km ( $70\text{--}140\text{ kg m}^{-2}\text{ a}^{-1}$ ); lower from 140 to 280 km ( $<46\text{ kg m}^{-2}\text{ a}^{-1}$ ); and medium from 280 to 500 km ( $46\text{--}70\text{ kg m}^{-2}\text{ a}^{-1}$ ). This pattern approximately coincides with the cane measurements along the line.

Based on the dating of the ice core at DT001 and density measurement, the history of the annual accumulation rates during the past 50 years is deduced (Fig. 7). The general trend at DT001 is slightly increasing, except for lower values in the decade 1957–67. But at MGA, western LGB, annual accumulation rates during the same period display an obviously decreasing trend. Although a decreasing accumulation rate has occasionally been reported (Graf and others, 1990; Kameda and others, 1990; Bindschadler and others, 1993), most studies reveal that accumulation rates have been increasing recently in Antarctica (Pouchet and others, 1983; Peel and Mulvaney, 1988; Morgan and others, 1991; Mosley-Thompson and others, 1995). This suggests a complexity, either in the spatial or in the temporal sense, of the accumulation-rate variation over the continent. The different accumulation rates on the two sides of the LGB may be attributable to the reciprocal relation of local circulation strength between the two sides.

### $\delta^{18}\text{O}$ – $T$ RELATIONSHIPS AND PAST CLIMATE

Figure 8 illustrates the relationships of  $\delta^{18}\text{O}$  vs mean annual temperature,  $T$ , of the two sides of the LGB. The plotted  $\delta^{18}\text{O}$  is the mean value in the upper 2 m of firn. Because of the lack of an integrated temperature series recorded by AWS, 10 m firn temperature ( $T_{10}$ ) was used as a substitute for mean annual temperature (Higham and Craven, 1997). Results from another coastal Antarctic transect, from Komsomolskaya to Mirny undertaken during the 1990 International Trans-Antarctic Expedition (ITAE; Qin and others, 1994), are also illustrated in Figure 8. It is clear that the  $\delta^{18}\text{O}$ – $T$  gradients on both sides of the LGB are different, with  $0.70\text{‰ }^{\circ}\text{C}^{-1}$  on the east side, and on the west side  $0.93\text{‰ }^{\circ}\text{C}^{-1}$ . The gradient on the west side is closer to that on the transect from Komsomolskaya to Mirny ( $0.90\text{‰ }^{\circ}\text{C}^{-1}$ ). On the whole,  $\delta^{18}\text{O}$  values in the Antarctic snow are dependent on the distance of vapor transport, but the topographic factor cannot be ignored since temperature and precipitation are different at various altitudes. Early studies have revealed that the  $\delta^{18}\text{O}$ – $T$  relationships are different in various regions of Ant-

arctica (Dansgaard and others, 1973; Lorius and Merlivat, 1977; Robin, 1983; Paterson, 1994; Qin and others, 1994). The  $\delta^{18}\text{O}$ – $T$  relationship is a key function used for the recovery of past climatic history from deep ice cores. The establishment of the function in different regions is necessary for precise interpretation of paleoclimate.

The different  $\delta^{18}\text{O}$ – $T$  relationships on the two sides of a glacier basin (LGB), an indicator of different meteorological regimes (Allison, 1998), confirm the necessity for widespread investigation of the  $\delta^{18}\text{O}$ – $T$  relationships in different areas of the Antarctic ice sheet. One must be extremely careful about using a single function for a wide area of the continent.

During the past 50 years, the  $\delta^{18}\text{O}$  profile at DT001 shows a slight increase, with a gradient of  $0.025\text{‰ a}^{-1}$ , which may imply an increase in air temperature (Fig. 7). Also, the gradient of the accumulation rate during this period increases by about  $0.39\text{ kg m}^{-2}\text{ a}^{-1}$ . The temperature trends, shown by the  $\delta^{18}\text{O}$  profiles in the ice cores at DT001 and MGA on opposite sides of the LGB, are different, with the east side showing an increase and the west side showing no obvious trend. This is similar to the relationship of the accumulation rates on the two sides. Temperature records from the weather stations at Mawson (west coast of LGB) and Davis (east coast of LGB) also reveal converse trends between the two stations (Jacka and Budd, 1998), with temperature increasing at Davis and decreasing at Mawson over recent decades. The declining tendency of temperature seems to go against the widespread acceptance that the climate has been warming over recent decades. As suggested by Jacka and Budd (1998), it may become possible to determine the interrelationships between the sea-ice and temperature changes by combining the archived climatic data for sea ice, atmosphere and ocean with modeling. In turn, this determination is important for understanding past climate records over decadal to centennial scales.

### CONCLUDING REMARKS

Primary results of glaciological investigations from three traverses, which cover a route that now totals 1128 km from Zhongshan station to Dome A, are presented. They are compared with the results obtained by Australian scientists from both sides of the LGB. Physical properties of the firn, such as density profiles, indicate that the densification process over Princess Elizabeth Land and Inaccessible Area is fairly slow. Comparison of accumulation rates,  $\delta^{18}\text{O}$ – $T$  relationships and  $\delta^{18}\text{O}$  profiles illustrates different relationships on either side of the LGB, both in a spatial and in a temporal sense. This may imply different climatic conditions on the two sides. However, the differences in accumulation and temperature over the past 50 years between the two sides are believed to be mainly due to the shifting of local circulation or sea-ice extent or their interaction. The comparison study in this area shows the necessity for careful, long-term investigations of complicated drainage areas such as the LGB, not only because of their significance for the accurate estimation of the mass balance of the ice sheet, but also because of their importance in revealing the real climate regime of Antarctica. This paper includes data from the first traverse plus a small amount from the second and third traverses. Most of the laboratory analyses and interpretations are still in progress, and more complete results are expected.

## ACKNOWLEDGEMENTS

The authors are grateful to the Chinese Polar Administration for logistic work for the inland traverses. This project was supported by the State Commission of Sciences and Technology of China (98-927), the Chinese Academy of Sciences (KZ951-A1-205) and the National Natural Science Foundation (49771022, 49971021).

## REFERENCES

- Allison, I. 1979. The mass budget of the Lambert Glacier drainage basin, Antarctica. *J. Glaciol.*, **22**(87), 223–235.
- Allison, I. 1998. Surface climate of the interior of the Lambert Glacier basin, Antarctica, from automatic weather station data. *Ann. Glaciol.*, **27**, 515–520.
- Bindschadler, R., P. L. Vornberger and S. Shabtaie. 1993. The detailed net mass balance of the ice plain on Ice Stream B, Antarctica: a geographic information system approach. *J. Glaciol.*, **39**(133), 471–482.
- Craven, M. and I. Allison. 1998. Firnification and the effects of wind-packing on Antarctic snow. *Ann. Glaciol.*, **27**, 239–245.
- Dansgaard, W., S. J. Johnsen, H. B. Clausen and N. Gundestrup. 1973. Stable isotope glaciology. *Medd. Grønl.*, **197**(2), 1–53.
- Goodwin, I. D., M. Higham, I. Allison and R. Jiawen. 1994. Accumulation variation in eastern Kemp Land, Antarctica. *Ann. Glaciol.*, **20**, 202–206.
- Graf, W., O. Reinwarth, H. Oerter and M. Dyurgerov. 1990. Isotopic and stratigraphical interpretation of a 16 m firn core nearby Druzhnaya I. In Miller, H., ed. *Filchner–Ronne–Ice–Shelf–Programme. Report No. 4 (1990)*. Bremerhaven, Alfred Wegener Institute for Polar and Marine Research, 46–49.
- Herron, M. 1982. Glaciochemical dating techniques. *Am. Chem. Soc. Symp. Ser.*, **176**, 303–318.
- Higham, M. and M. Craven. 1997. *Surface mass balance and snow surface properties from the Lambert Glacier basin traverses 1990–94*. Hobart, Tasmania, Cooperative Research Centre for the Antarctic and Southern Ocean Environment. (Research Report 9)
- Higham, M., M. Craven, A. Ruddell and I. Allison. 1997. Snow-accumulation distribution in the interior of the Lambert Glacier basin, Antarctica. *Ann. Glaciol.*, **25**, 412–417.
- Jacka, T. H. and W. F. Budd. 1998. Detection of temperature and sea-ice-extent changes in the Antarctic and Southern Ocean, 1949–96. *Ann. Glaciol.*, **27**, 553–559.
- Kameda, T., M. Nakawo, S. Mae, O. Watanabe and R. Naruse. 1990. Thinning of the ice sheet estimated from total gas content of ice cores in Mizuho Plateau, East Antarctica. *Ann. Glaciol.*, **14**, 131–135.
- Lorius, C. and L. Merlivat. 1977. Distribution of mean surface stable isotope values in East Antarctica: observed changes with depth in the coastal area. *International Association of Hydrological Sciences Publication 118 (Symposium at Grenoble 1975 — Isotopes and Impurities in Snow and Ice)*, 127–137.
- McIntyre, N. F. 1985. A re-assessment of the mass balance of the Lambert Glacier drainage basin, Antarctica. *J. Glaciol.*, **31**(107), 34–38.
- Morgan, V. I., I. D. Goodwin, D. M. Etheridge and C. W. Wookey. 1991. Evidence from Antarctic ice cores for recent increases in snow accumulation. *Nature*, **354**(6348), 58–60.
- Mosley-Thompson, E. and 6 others. 1995. Recent increase in South Pole snow accumulation. *Ann. Glaciol.*, **21**, 131–138.
- Paterson, W. S. B. 1994. *The physics of glaciers. Third edition*. Oxford, etc., Elsevier.
- Peel, D. A. and R. Mulvaney. 1988. Air temperature and snow accumulation in the Antarctic Peninsula during the past 50 years. (Abstract) *Ann. Glaciol.*, **11**, 207.
- Pourchet, M., J. F. Pinglot and C. Lorius. 1983. Some meteorological applications of radioactive fallout measurements in Antarctic snows. *J. Geophys. Res.*, **88**(C10), 6013–6020.
- Qin Dahe. 1990. Densification process within the near-surface layer of the Antarctic ice sheet. *Antarct. Res.*, **2**(1), 10–19.
- Qin Dahe, J. R. Petit, J. Jouzel and M. Stievenard. 1994. Distribution of stable isotopes in surface snow along the route of the 1990 International Trans-Antarctica Expedition. *J. Glaciol.*, **40**(134), 107–118.
- Ren Jiawen, Qin Dahe and I. Allison. 1999. Variations of snow accumulation and temperature over past decades in the Lambert Glacier basin, Antarctica. *Ann. Glaciol.*, **29**, 29–32.
- Robin, G. de Q. 1983. *The climatic record in polar ice sheets*. Cambridge, etc., Cambridge University Press.